BIT Numer Math (2012) 52:981–1007
DOI 10.1007/s10543-012-0382-4
BIT

Fully discrete semi-Lagrangian methods for advection of differential forms

Holger Heumann · Ralf Hiptmair · Kun Li · Jinchao Xu

Received: 16 April 2011 / Accepted: 21 March 2012 / Published online: 17 April 2012

Abstract We study the discretization of linear transient transport problems for differential forms on bounded domains. The focus is on unconditionally stable semi-Lagrangian methods that employ finite element approximation on fixed meshes combined with tracking of the flow map. We derive these methods as finite element Galerkin approach to discrete material derivatives and discuss further approximations leading to fully discrete schemes.

We establish comprehensive a priori error estimates, in particular a new asymptotic estimate of order $O(h^{r+1}\tau^{-\frac{1}{2}})$ for the L^2-error of semi-Lagrangian schemes with exact L^2-projection. Here, h is the spatial meshwidth, τ denotes the timestep, and r is the (full) polynomial degree of the piecewise polynomial discrete differential forms used as trial functions. Yet, numerical experiments hint that the estimates may still be sub-optimal for spatial discretization with lowest order discrete differential forms.

Keywords Advection-diffusion problem · Discrete differential forms · Discrete Lie derivative · Semi-Lagrangian methods

Mathematics Subject Classification 65M60 · 65M25

Communicated by Rolf Stenberg.

H. Heumann · R. Hiptmair (✉)
Seminar for Applied Mathematics, Swiss Federal Institute of Technology, Zurich, Switzerland
e-mail: hiptmair@sam.math.ethz.ch

K. Li
School of Mathematical Sciences, Peking University, Beijing, China

J. Xu
Department of Mathematics, Penn State University, University Park, USA

1 Introduction

We deal with transport dominated boundary value problems set in a bounded polyhedral Lipschitz domain $\Omega \subset \mathbb{R}^n$ (with unit outward normal $\boldsymbol{n}$) and governed by a *prescribed* uniformly Lipschitz continuous stationary velocity vector field $\boldsymbol{\beta} : \overline{\Omega} \mapsto \mathbb{R}^n$. To avoid technical difficulties we *assume* throughout

$$\boldsymbol{\beta} \cdot \boldsymbol{n} = 0 \quad \text{on } \partial\Omega, \tag{A.1}$$

that is, $\boldsymbol{\beta}$ has vanishing normal components on the boundary of Ω.

Next, recall the classical linear transient 2nd-order advection-diffusion problem for an unknown scalar function $u = u(x, t)$:

$$\begin{aligned} \partial_t u + \boldsymbol{\beta} \cdot \mathbf{grad}\, u - \varepsilon\, \mathsf{div}\, \mathbf{grad}\, u &= f \qquad \text{in } \Omega \times]0, T[, \\ u &= 0 \qquad \text{on } \partial\Omega \times]0, T[, \\ u(\cdot, 0) &= u_0. \end{aligned} \tag{1.1}$$

Here, $f \in C^1([0, T]; L^2(\Omega))$ models a source and u_0 provides initial data. The parameter $\varepsilon \geq 0$ controls the strength of diffusion; for $0 < \varepsilon \ll 1$ the boundary value problem qualifies as *advection-dominated*.

Solving such advection-diffusion problems numerically is challenging in the case of dominant advection, because we encounter a singular perturbation. In the limit $\varepsilon \to 0$ of vanishing diffusion the problem type changes from parabolic to hyperbolic, and the standard methods for parabolic problems usually fail.

We can distinguish two main families of methods for tackling the limiting transport problem: Eulerian methods and Lagrangian methods. The former rely on spatial discretization on a fixed mesh, to which some numerical timestepping procedure is applied. Convergence and stability are guaranteed by adding certain stabilization terms as in e.g. SUPG finite element methods [23] or discontinuous Galerkin method with upwind fluxes [22, 26, 33]. Conversely, Lagrangian methods dispense with a fixed spatial mesh and approximately track the flow induced by the velocity $\boldsymbol{\beta}$. Typical representatives are methods based on characteristics [4, 11, 34] and many kinds of particle methods [9].

Both principles are blended in the semi-Lagrangian approach, which is the focus of this article. On the one hand, it relies on fixed spatial meshes. On the other hand, transport is taken into account through explicit use of the flow map. Many variants of semi-Lagrangian methods for (1.1) (often for the case $\varepsilon = 0$) have been proposed and analyzed in a large number of research papers, see, e.g., [10, 12, 28, 31]. A review of the literature is given in [17, Sect. 5].

This article is concerned with the numerical analysis of semi-Lagrangian methods, as well, but its scope extends beyond the boundary value problem (1.1), because we look at it from the perspective of differential forms on the n-dimensional manifold Ω. Then, utilizing the notion of the *Lie derivative*, (1.1) turns out to be the particular instance for $p = 0$ of the following generalized advection-diffusion problems for time

dependent differential p-forms $\omega = \omega(t)$, $0 \le p \le n$,

$$\begin{aligned} *\partial_t \omega + *L_{\boldsymbol{\beta}} \omega + \varepsilon(-1)^{p+1} d * d\omega &= \varphi(t) \quad \text{in } \Omega \times (0,T), \\ \iota^* \omega &= 0 \quad \text{on } \partial\Omega \times (0,T), \\ \omega(0) &= \omega_0. \end{aligned} \tag{1.2}$$

Here, d is the exterior derivative and $*$ is the Hodge operator and ι^* stands for the trace of a differential form. The advection operator $L_{\boldsymbol{\beta}}$ is the Lie derivative [13, p. 133] for the prescribed velocity field $\boldsymbol{\beta}$. More explanations will be given in the next section. Extra details and an introduction to the calculus of differential forms in the context of discretization of partial differential equations are given in [21, Sect. 2], [1, Sect. 2], and [2, Sect. 4].

The connection between (1.2) and (1.1) is established through the concept of *Euclidean vector proxies*, which allows to model p-forms on Ω through vector fields with $\binom{n}{p}$ components, see [7, Sect. 7], [1, Table 2.1], and [21, Table 2.1].[1] For vector proxies in 3D the exterior derivative is incarnated by the classical differential operators **grad**, **curl**, and div.

A first benefit of studying the boundary value problem (1.2) is that, apart from (1.1) for $p = 0$, for $p = 1$ it also comprises the so-called magnetic advection-diffusion problem arising in quasistatic electromagnetic models in the presence of moving media, see [18, Sect. 5]. In vector proxy notation the corresponding PDE reads

$$\partial_t \boldsymbol{A} + \mathbf{curl}\, \boldsymbol{A} \times \boldsymbol{\beta} + \mathbf{grad}(\boldsymbol{\beta} \cdot \boldsymbol{A}) + \varepsilon\, \mathbf{curl}\,\mathbf{curl}\, \boldsymbol{A} = \boldsymbol{f}. \tag{1.3}$$

This vectorial advection-diffusion equation is a building block for models of magnetohydrodynamics (MHD).

Another benefit of the perspective of differential forms is the possibility of a unified treatment of the various cases $p = 0, \ldots, n$. This is complemented by the big advantage of the calculus of differential forms to reveal intrinsic structure, which might be blurred by the "metric overhead" carried by vector calculus.

The use of discrete differential forms for the Galerkin discretization of the diffusion operator $d * d\omega$ in (1.2) is well understood by now [1, Chap. 7]. Here, our main interest is in *robustness* of the methods, that is, their sustained performance in the case $\varepsilon \to 0$. The guideline is that robustness can only be expected, if the method remains viable for the limit case $\varepsilon = 0$. Therefore, we will examine the proposed semi-Lagrangian methods only for the pure advection problem

$$\begin{aligned} *\partial_t \omega(t) + *L_{\boldsymbol{\beta}} \omega(t) &= \varphi(t) \quad \text{in } \Omega \times]0,T[, \\ \omega(0) &= \omega_0. \end{aligned} \tag{1.4}$$

Note that thanks to (A.1) no inflow is possible and, thus, no boundary conditions on $\partial\Omega$ are needed.

[1] Occasionally we will use the operator v. p. to indicate that a form is mapped to its corresponding Euclidean vector proxy.

In Sects. 2 and 3 below we recall the derivation of the semi-Lagrangian discretization of (1.4). Of course, for scalar problems, e.g. $p = 0$, the methods will resemble the known semi-Lagrange Galerkin schemes [10, 31] and semi-Lagrangian schemes based on interpolation [37].

The core part of the paper will then be devoted to convergence analysis and numerical studies. We start with the abstract convergence theorem Theorem 4.1 in Sect. 4 that provides a priori error estimates in terms of meshwidth h and timestep size τ. We point out that its application to concrete variants of semi-Lagrangian schemes for $p = 0$ reproduces known convergence results [10, 28, 31]. However, for the simplest lowest order discrete p-forms, $p > 0$, Theorem 4.1 does not predict convergence in the $L^2(\Omega)$-norm, when spatial and temporal resolution are increased in tandem. A refined convergence theory for semi-Lagrangian methods based on L^2-projection is presented in Theorem 4.2 inspired by an argument from [25].

Subsequently, in Sect. 5, we study fully discrete schemes that involve approximate characteristics. For them we also prove a priori error estimates in terms of meshwidth h and timestep size τ (for fixed polynomial degree of discrete forms). Finally, numerical experiments for 1-forms are reported in Sect. 6. Results for scalar advection ($p = 0$) are reported in [19].

Notations Regard Ω as a smooth, compact, oriented, n-dimensional Riemannian manifold with boundary. Now we write $\mathcal{F}^p(\Omega)$ for the space of smooth p-forms on Ω. A smooth differential form ω assigns to each point $x \in \Omega$ and p vectors $\boldsymbol{v}_1, \ldots, \boldsymbol{v}_p$ from the tangent space at x a number. For x fixed a smooth differential form ω induces a p-linear alternating mapping ω_x on the tangent space at x [36].

Completion of $\mathcal{F}^p(\Omega)$ in the norm $\|\omega\|_0 := \int_\Omega \omega \wedge *\omega$ yields the Hilbert space $L^{2,p}(\Omega)$ of L^2-integrable differential p-forms, whose inner product we are going to denote by $(\cdot,\cdot)_\Omega$. Analogously to the Sobolev spaces $H^m(\Omega)$ and $W^{m,q}(\Omega)$ for scalar functions with $m > 0$ derivatives in $L^2(\Omega)$ and $L^q(\Omega)$ [36, Sect. 1.3] we define Sobolev-spaces $W^{m,q,p}$ and $H^{m,p}$ for differential forms by requiring that the map

$$x \mapsto \omega_x\big(\boldsymbol{v}_1(x), \ldots, \boldsymbol{v}_p(x)\big) \tag{1.5}$$

gives rise to a function in $W^{m,q}(\Omega)$ and $H^m(\Omega)$, where $\boldsymbol{v}_1(x), \ldots, \boldsymbol{v}_p(x)$ are smooth vector fields on Ω. In the following we will frequently omit the index p in $L^{2,p}(\Omega)$, $W^{m,q,p}(\Omega)$ and $H^{m,p}(\Omega)$ and denote by $\|\cdot\|_{m,q}$ ($|\cdot|_{m,q}$) and $\|\cdot\|_m$ ($|\cdot|_m$) the corresponding (semi)-norms. We also use the standard notations $\mathbf{W}^{m,q}(\Omega)$, $|\boldsymbol{\beta}|_{\mathbf{W}^{m,q}(\Omega)}$ and $\|\boldsymbol{\beta}\|_{\mathbf{W}^{m,q}(\Omega)}$ to denote Sobolev spaces, Sobolev semi-norms and Sobolev norms of vector valued functions with $m > 0$ derivatives in $L^q(\Omega)$. We may omit the domain of integration when it is clear from the context.

2 Lie derivatives and material derivatives of forms

We introduce the space-time domain $Q_T := \Omega \times [0, T]$, $T > 0$. We write $(x, t) \mapsto X_t(x)$, $t \in \mathbb{R}$, $x \in \Omega$, for the flow map associated with the stationary continuous velocity field $\boldsymbol{\beta} : \overline{\Omega} \mapsto \mathbb{R}^n$, $\boldsymbol{\beta} \in \mathbf{W}^{1,\infty}(\Omega)$, that is

$$\frac{d}{dt} X_t(x) = \boldsymbol{\beta}\big(X_t(x)\big) \quad \forall x \in \Omega,\ t \in \mathbb{R}, \qquad X_0(x) = x. \tag{2.1}$$

The flow map is time-reversible, that is

$$X_t \circ X_{-t} = \mathrm{id} \quad \forall t \in \mathbb{R}. \tag{2.2}$$

Before introducing the Lie derivative we recall the definition of the directional derivative for scalar functions $f : \Omega \mapsto \mathbb{R}$:

$$(\boldsymbol{\beta} \cdot \mathbf{grad}\, f)(x) := \lim_{t \to 0} \frac{f(X_t(x)) - f(x)}{t}. \tag{2.3}$$

Scalar functions can be viewed as 0-forms and the Lie derivative $L_{\boldsymbol{\beta}}$ of higher p-form $\omega \in \mathcal{F}^p(\Omega)$ turns out to be the generalization of the directional derivative for a scalar function. For differential forms $\omega \in \mathcal{F}^p(\Omega)$ of order p, $p > 0$, we replace the point evaluation of 0-forms with integration over p-dimensional oriented sub-manifolds M_p of Ω. Then the Lie derivative of a p-form ω is [13, Chap. 4]:

$$\int_{M_p} L_{\boldsymbol{\beta}} \omega := \lim_{t \to 0} \frac{1}{t} \left(\int_{X_t(M_p)} \omega - \int_{M_p} \omega \right). \tag{2.4}$$

In terms of the pullback X_t^* with

$$\int_{M_p} X_t^* \omega := \int_{X_t(M_p)} \omega \tag{2.5}$$

we can also write

$$L_{\boldsymbol{\beta}} \omega := \lim_{t \to 0} \frac{X_t^* \omega - \omega}{t}. \tag{2.6}$$

We refer to [6, p. 26] and [20, Remarks 1.1, 1.2] for vector proxy representations of Lie derivatives in two and three dimensional Euclidean space.

Taking into account the time dependence of the differential form $\omega = \omega(t)$, the limit value of (2.6) yields the so called *material derivative*:

$$D_{\boldsymbol{\beta}} \omega(t) := \lim_{\tau \to 0} \frac{X_\tau^* \omega(t + \tau) - \omega(t)}{\tau}. \tag{2.7}$$

This derivative is the rate of change of the action of differential forms in moving media [14, p. 62]. We deduce:

$$\begin{aligned} D_{\boldsymbol{\beta}} \omega(t) &= \lim_{\tau \to 0} \frac{X_\tau^* \omega(t + \tau) - X_\tau^* \omega(t)}{\tau} + \lim_{\tau \to 0} \frac{X_\tau^* \omega(t) - \omega(t)}{\tau} \\ &= \frac{\partial}{\partial t} \omega(t) + L_{\boldsymbol{\beta}} \omega(t). \end{aligned} \tag{2.8}$$

In conclusion we see that our limit problem (1.4) is a transport problem:

$$D_{\boldsymbol{\beta}} \omega(t) = \widetilde{\varphi}(t) \quad \text{in } Q_T, \qquad \omega(0) = \omega_0, \tag{2.9}$$

with $\widetilde{\varphi} := (-1)^{n(n-p)} * \varphi$, since $** \omega = (-1)^{n(n-p)}\omega$ [13, p. 364]. The explicit solution of this transport problem (2.9) follows from semi-group theory:

$$\omega(t) = X_{-t}^{*}\omega(0) + \int_0^t \left(X_{\tau-t}^{*}\widetilde{\varphi}(\tau)\right) d\tau. \tag{2.10}$$

For $\varphi = 0$ this means, that the advected p-form ω evaluated at time t on some p-dimensional manifold M_p is equal to the value of ω at time 0 on the manifold $X_{-t}(M_p)$, i.e. the image of M_p under X_{-t}.

Remark 2.1 In the case $\varphi = 0$ we find the following key conservation properties of the solution of (2.9):

First, closed forms remain closed when they are advected by the material derivative; if $D_{\boldsymbol{\beta}}\omega(t) = 0$ and $d\omega(0) = 0$ then $d\omega(t) = 0$, $\forall t$. This is a simple consequence of the fact that the material derivative and the exterior derivative commute $D_{\boldsymbol{\beta}} d = d D_{\boldsymbol{\beta}}$.

Second, the so-called helicity is a conserved quantity of the solution of (1.4). If n is odd and $p = \frac{n-1}{2}$, then

$$h_1\big(\omega(0)\big) = h_1\big(\omega(t)\big) := \int_\Omega d\omega(t) \wedge \omega(t) \tag{2.11}$$

for solutions of (2.9). If n is even and $p = \frac{n}{2}$, then we find conservation

$$h_2\big(\omega(0)\big) = h_2\big(\omega(t)\big) := \int_\Omega \omega(t) \wedge \omega(t), \quad \forall t \tag{2.12}$$

and

$$h_3\big(\omega(0)\big) = h_3\big(\omega(t)\big) := \int_\Omega d\omega(t) \wedge i_{\boldsymbol{\beta}}\omega(t), \quad \forall t. \tag{2.13}$$

For Euclidean vector proxies $\boldsymbol{A}(t)$ of time-dependent 1-forms in $\mathbb{R}^3$ the helicity functional has the familiar form

$$h_1\big(\boldsymbol{A}(t)\big) = \int_\Omega \mathbf{curl}\, \boldsymbol{A}(t) \cdot \boldsymbol{A}(t)\, d\boldsymbol{x}.$$

The proof of (2.11), (2.12) and (2.13) follows from the Leibniz rule for Lie derivatives of products of p-forms ω and $n - p$ forms η [13, p. 133]:

$$d i_{\boldsymbol{\beta}}(\omega \wedge \eta) = L_{\boldsymbol{\beta}}(\omega \wedge \eta) = L_{\boldsymbol{\beta}}\omega \wedge \eta + \omega \wedge L_{\boldsymbol{\beta}} \tag{2.14}$$

and the assumption that the velocity field $\boldsymbol{\beta}$ has vanishing normal components on the boundary of Ω.

It goes without saying that it is very desirable to design numerical algorithms that inherit these properties and preserve closedness and helicity exactly or at least in some approximative sense.

3 Discrete differential forms

Let $\Omega_h = \{T\}$ be some simplicial triangulation of Ω, possibly comprising curvilinear elements in order to resolve $\partial\Omega$. For $T \in \Omega_h$, h_T denotes the diameter and $h = \max_{T\in\Omega_h} h_T$. Our approach to the discretization of (2.9) seeks to approximate $\omega(t)$ for certain times t_k in a (fixed) space of *discrete differential forms* that are piecewise polynomial on Ω_h.

Finite element spaces for differential forms of arbitrary polynomial degree are available. There are two main families, designated by $\mathcal{W}_r^p(\Omega_h)$, with $0 < p \leq n$ and $r \in \mathbb{N}_0$, and $\check{\mathcal{W}}_r^p(\Omega_h)$, with $0 \leq p < n$ and $r \in \mathbb{N}$, respectively, see [21, pp. 271, 272], [1, Sect. 5], [2, Sect. 5]. Here r is related to the local polynomial degree and tells us that the complete spaces of polynomials forms of degree r are contained in the local spaces on each simplex.

Forms in both these families of finite element spaces have a well-defined exterior derivative $\in L^{2,p+1}(\Omega)$. Further, for both families there exist so-called canonical nodal interpolation operators $I_h^p : \mathcal{F}^p(\Omega) \mapsto \mathcal{W}_r^p(\Omega_h)/\check{\mathcal{W}}_r^p(\Omega_h)$ [1, p. 62] commuting with the exterior derivative

$$d I_h^p \omega = I_h^{p+1} d\omega, \quad \text{for all smooth } p\text{-forms } \omega \text{ on } \Omega. \tag{3.1}$$

The interpolation operators I_h^p are built on canonical moment-based degrees of freedom of the finite element spaces $\mathcal{W}_r^p(\Omega_h)$ and $\check{\mathcal{W}}_r^p(\Omega_h)$, see [21, Sect. 3.4]. In the lowest order case of $\mathcal{W}_0^p(\Omega_h)$ these are simply the integrals $\int_{M_p} \omega$ on all p-dimensional facets M_p of all elements $T \in \Omega_h$.

In $\mathbb{R}^3$ and $\mathbb{R}^2$ the spaces $\mathcal{W}_r^p(\Omega_h)$ and $\check{\mathcal{W}}_r^p(\Omega_h)$ agree with known classical finite element spaces [1, p. 60] when we consider Euclidean vector proxies. For example, in $\mathbb{R}^3$ the spaces $\mathcal{W}_r^1(\Omega_h)$ and $\check{\mathcal{W}}_r^1(\Omega)$ are Nédélec's 1st and 2nd family of edge elements presented in [29] and [30].

Subsequently, we adopt the unified notation $\mathcal{W}^p(\Omega_h)$ for a generic space of piecewise polynomial discrete differential forms on Ω_h contained in $L^{2,p}(\Omega)$. It may stand for either $\mathcal{W}_r^p(\Omega_h)$ or $\check{\mathcal{W}}_r^p(\Omega_h)$. In any case, $r \in \mathbb{N}_0$ will denote the *maximal* degree of polynomial forms *completely* contained in the local spaces of $\mathcal{W}^p(\Omega_h)$. Thus, we can rely on the following standard best approximation estimates

$$\inf_{\omega_h \in \mathcal{W}^p} \|\omega - \omega_h\|_{0,q} \leq C h^{\min(s,r+1)} |\omega|_{s,q} \quad \forall \omega \in W^{s,q,p}(\Omega), \tag{3.2}$$

for $s \in \mathbb{N}$, $1 \leq q \leq \infty$, $0 < p \leq n$, with $C > 0$ independent of h [1, Theorem 5.3].

Remark 3.1 We point out that semi-Lagrangian schemes for pure advection do not rely on well-defined exterior derivatives of forms in $\mathcal{W}^p(\Omega_h)$. Yet, in light of the conserved quantities of Remark 2.1 helicity, we consider it reasonable to look for discretizations in such spaces of discrete differential forms, for which the exterior derivative can be defined as an $L^2(\Omega)$-differential form globally. Moreover, when a diffusion term has to be dealt with, this property is required for its standard Galerkin discretization.

4 Semi-Lagrangian discretization

The pullback $X_{-\tau}^* \omega_h$ of a discrete differential form $\omega_h \in \mathcal{W}^p(\Omega_h)$ will usually fail to belong to $\mathcal{W}^p(\Omega_h)$. Thus, in order to convert the solution formula (2.10) into a timestepping scheme for discrete differential forms, we need to introduce an intermediate projection $P_h^p : \mathcal{F}^p(\Omega) \mapsto \mathcal{W}^p(\Omega_h)$ mapping the pullback of discrete differential forms back to the discrete space. Given such an abstract projection operator, the discrete semi-Lagrangian timestepping scheme with uniform timestep $\tau = \frac{T}{N}$, $N \in \mathbb{N}$, generates approximations ω_h^i to $\omega(i\tau)$ by the recursion

$$\begin{aligned} \omega_h^0 &= P_h^p \omega_0; \\ \omega_h^{i+1} &= P_h^p X_{-\tau}^* \omega_h^i + P_h^p \int_{t_i}^{t_{i+1}} X_{s-t_{i+1}}^* \widetilde{\varphi}(s)\, ds, \quad i = 0, \ldots, N-1. \end{aligned} \tag{4.1}$$

Here, we first give an abstract error analysis for this semi-Lagrangian scheme (4.1), under the assumption that the effect of the pullback can be controlled according to

$$\left\| X_{-\tau}^* \omega \right\|_{0,q} \leq (1 + C_e \tau) \|\omega\|_{0,q}, \tag{4.2}$$

with a constant $C_e > 0$. Here and in the sequel all constants may only depend on Ω, the shape-regularity of the mesh Ω_h, and the norms occurring in estimates. We also assume a contraction property of the projection

$$\left\| P_h^p \omega \right\|_{0,q} \leq \|\omega\|_{0,q}. \tag{4.3}$$

Theorem 4.1 (See, e.g., [28, 38] for $p = 0$) *Let $\omega \in W^{s,q}(\Omega)$ and $\omega_h \in \mathcal{W}^p(\Omega_h)$ be the solutions of (1.4) and (4.1). Further assume that*

$$\left\| P_h^p \omega - \omega \right\|_{0,q} \leq C_p h^{\min(s, r+1)} \|\omega\|_{s,q} \quad \forall \omega \in W^{s,q}(\Omega) \tag{4.4}$$

for some $1 \leq q \leq \infty$ and $s > 0$. If (4.2) and (4.3) hold, then

$$\max_{0 \leq i \leq N} \left\| \omega^i - \omega_h^i \right\|_{0,q} \leq C h^{\min(s, r+1)} \left(\frac{1}{\tau} + 1 \right) \max_{0 \leq n \leq N} \left\| \omega^n \right\|_{s,q},$$

where $\omega^i = \omega(i\tau)$ and $C > 0$ is independent of h and τ.

Proof To bound the error $\|\omega^i - \omega_h^i\|_{0,q}$ we add and subtract the projection $P_h^p \omega^i$, use Cauchy-Schwarz and formulas (1.4) and (4.1):

$$\begin{aligned} \left\| \omega^i - \omega_h^i \right\|_{0,q} &\leq \left\| \omega^i - P_h^p \omega^i \right\|_{0,q} + \left\| P_h^p \omega^i - \omega_h^i \right\|_{0,q} \\ &\leq \left\| \omega^i - P_h^p \omega^i \right\|_{0,q} + \left\| P_h^p X_{-\tau}^* \omega^{i-1} - P_h^p X_{-\tau}^* \omega_h^{i-1} \right\|_{0,q} \\ &\leq \left\| \omega^i - P_h^p \omega^i \right\|_{0,q} + (1 + C_e \tau) \left\| \omega^{i-1} - \omega_h^{i-1} \right\|_{0,q}. \end{aligned}$$

The last inequality follows from assumptions (4.2) and (4.3). A discrete Gronwall-like inequality and the approximation assumption (4.4) yield with $m := \min(s, r+1)$

$$\begin{aligned}\left\|\omega^i - \omega_h^i\right\|_{0,q} &\leq \frac{\exp(C_e\tau i)-1}{C_e\tau} \max_{0\leq n<i} \left\|\omega^n - P_h^p\omega^n\right\|_{0,q} + \left\|\omega^i - \omega_h^i\right\|_{0,q} \\ &\leq C_p \frac{\exp(C_e\tau i)-1}{C_e\tau} h^m \max_{0\leq n<i} \left\|\omega^n\right\|_{s,q} + C_p \left\|\omega^i\right\|_{s,q},\end{aligned}$$

and the assertion follows. □

Note that no conditions on the timestep size τ are imposed in Theorem 4.1, which bears out the *unconditional stability* of semi-Lagrangian schemes in the case of large timesteps, provided that the underlying projection is a contraction, cf. [27].

Remark 4.1 However, the bounds in Theorem 4.1 blow up when keeping the mesh fixed and letting the timestep $\tau \to 0$. Almost all theoretical estimates for semi-Lagrangian methods for scalar advection yield bounds that involve a negative power of τ, with the exception of the result in [28, Theorem 2.1, p. 339]. With the techniques devised in that article one can show for $p = 0$, $\mathcal{W}^0(\Omega) \subset C^0(\overline{\Omega})$, and sufficiently smooth ω that under the assumptions of the theorem

$$\max_{0\leq i\leq N} \left\|\omega^i - \omega_h^i\right\|_{0,q} \leq C h^{\min(s,r+1)} \left(\frac{1}{h}+1\right) \max_{0\leq n\leq N} \left\|\omega^n\right\|_{s,q}, \tag{4.5}$$

for all $h > 0$ and $\tau > 0$. This rules out blow-up for timestep $\tau \to 0$. For the case $p = n$ Theorem 3.1 in [28] establishes a similar estimate in the L^1-norm. The general case is an open problem.

Next, we examine two concrete choices of the abstract projection operator P_h^p.

(1) *Interpolation scheme*. Natural projection operators are the standard nodal interpolation operators I_h^p for discrete differential forms, see Sect. 3. With these, the *interpolation* based semi-Lagrangian scheme reads:

$$\begin{aligned}\omega_h^0 &= I_h^p \omega_0; \\ \omega_h^{i+1} &= I_h^p X_{-\tau}^* \omega_h^i + \int_{t_i}^{t_{i+1}} I_h^p X_{s-t_{i+1}}^* \widetilde{\varphi}(s)\, ds.\end{aligned} \tag{4.6}$$

Unfortunately, Theorem 4.1 does not give convergence for most of these schemes, since the interpolation operator lacks continuity in $L^q(\Omega)$. Only for the lowest order approximation of 0-forms (functions), e.g. $\mathcal{W}^0(\Omega_h) = \check{\mathcal{W}}_1^0(\Omega_h)$, and $q = \infty$, we have the contraction property

$$\left\|I_h^0 u\right\|_{0,\infty} \leq \|u\|_{0,\infty} \quad \forall u \in L^\infty(\Omega) \cap C^0(\Omega),$$

because I_h boils down to nodal interpolation onto piecewise linear functions. Then the arguments of Theorem 4.1 carry over and establish convergence in the

L^∞-norm according to

$$\max_{0\le i\le N} \left\|\omega^i - \omega_h^i\right\|_{0,\infty} \le Ch^{\min(s,2)}\left(\frac{1}{\tau}+1\right)\max_{0\le n\le N}\left\|\omega^n\right\|_{s,\infty}.$$

Nevertheless in our 2D experiments the interpolation scheme for $p=1$ invariably converged in $L^2(\Omega)$, see Sect. 6.

Remark 4.2 Thanks to their commuting diagram property (3.1) the interpolation operators I_h^p map closed forms to closed discrete forms. As a consequence the semi-Lagrangian scheme (4.6) also preserves closedness in the sense that

$$d\omega(0)=0 \quad \text{and} \quad d\widetilde{\varphi}=0 \quad \Rightarrow \quad d\omega_h^i=0 \quad \forall i.$$

(2) *Galerkin projection scheme*. The L^2-orthogonal projection operator Π_h^p defined by

$$\left(\Pi_h^p\omega,\eta_h\right)_\Omega := (\omega,\eta_h)_\Omega \quad \omega\in\mathcal{F}^p(\Omega),\eta_h\in\mathcal{W}^p(\Omega_h), \tag{4.7}$$

is another natural candidate for the abstract projection operator in (4.1). The resulting *Galerkin projection* semi-Lagrangian scheme reads:

$$\begin{aligned}
&\left(\omega_h^0,\eta_h\right)_\Omega = (\omega_0,\eta_h)_\Omega \quad \forall\eta_h\in\mathcal{W}^p(\Omega_h);\\
&\left(\omega_h^{i+1},\eta_h\right)_\Omega = \left(X_{-\tau}^*\omega_h^i,\eta_h\right)_\Omega + \int_{t_i}^{t_{i+1}}\left(X_{s-t_{i+1}}^*\widetilde{\varphi}(s),\eta_h\right)_\Omega ds \quad \forall\eta_h\in\mathcal{W}^p(\Omega_h).
\end{aligned} \tag{4.8}$$

First, as is readily seen, the L^2-projection Π_h^p commutes with integration in time. Second, we clearly have a contraction property $\|\Pi_h^p\|_0\le 1$ for the projection operator, and the best approximation estimates (3.2) for $q=2$ immediately yield analogous estimates for Π_h^p. Hence, Theorem 4.1 gives convergence once the bounded expansion property (4.2) of $\|X_{-\tau}^*\omega\|_0$ is verified. The assumption that $\boldsymbol{\beta}$ has vanishing normal components implies $X_\tau(\Omega)=\Omega$ and thus

$$\left\|X_{-\tau}^*\omega\right\|_0 = \int_\Omega X_{-\tau}^*\omega\wedge *X_{-\tau}^*\omega = \int_\Omega \omega\wedge X_\tau^**X_{-\tau}^*\omega. \tag{4.9}$$

In the cases $n=2$ and $n=3$ we can immediately deduce explicit representations of $X_\tau^**X_{-\tau}^*$ from the known representation formulas for pullbacks (see [21, p. 245]), e.g. for differential forms ω in $\mathbb{R}^3$ with vector proxies u or $\boldsymbol{u}$ we get:

$$\begin{aligned}
p=0:&\quad \text{v.p.}\left(X_\tau^**X_{-\tau}^*\omega\right)(x) = \det\left(DX_\tau(x)\right)u(x),\\
p=1:&\quad \text{v.p.}\left(X_\tau^**X_{-\tau}^*\omega\right)(x) = \det\left(DX_\tau(x)\right)DX_\tau^{-1}(x)DX_\tau^{-T}(x)\boldsymbol{u}(x),\\
p=2:&\quad \text{v.p.}\left(X_\tau^**X_{-\tau}^*\omega\right)(x) = \det\left(DX_\tau(x)\right)^{-1}DX_\tau^{T}(x)DX_\tau(x)\boldsymbol{u}(x),\\
p=3:&\quad \text{v.p.}\left(X_\tau^**X_{-\tau}^*\omega\right)(x) = \det\left(DX_\tau(x)\right)^{-1}u(x).
\end{aligned} \tag{4.10}$$

In summary, we can bound $X^*_{-\tau}\omega$ by

$$\left\|X^*_{-\tau}\omega\right\|_0^2 \le C(\tau)\|\omega\|_0^2, \tag{4.11}$$

where the constant $C(\tau)$, with $C(0) = 1$, depends on the Jacobian DX_τ and determinant $\det(DX_\tau)$. For smooth velocity $\boldsymbol{\beta}$ these are smooth functions of τ [15, p. 100], thus, Taylor expansion and $DX_0 = \mathrm{Id}$, yield the desired bound for sufficiently small τ:

$$\left\|X^*_{-\tau}\omega\right\|_0^2 \le (1 + C_e\tau)\|\omega\|_0^2. \tag{4.12}$$

For the general case of p-forms in $\mathbb{R}^n$ similar bounds can be established according to the following lemma. Its proof is based on the observation is that the quantity $X^*_\tau * X^*_{-\tau}$ encodes a perturbation of the standard metric that is related to the Hodge operator $*$. For smooth $\boldsymbol{\beta}$ also this perturbation depends smoothly on τ.

Lemma 4.1 *If $\boldsymbol{\beta} \in \mathbf{W}^{1,\infty}(\Omega)$ satisfies Assumption* (A.1), *we can bound*

$$\left\|X^*_{-\tau}\omega\right\|_0^2 \le (1 + C_e\tau)\|\omega\|_0^2 \quad \forall\omega \in L^2(\Omega), \tag{4.13}$$

with $C_e = C_e(\|\boldsymbol{\beta}\|_{1,\infty}) > 0$ independent of τ.

Proof We closely follow the proof of Proposition A.1 in [17] and first show

$$\int_{X_\tau(\Omega)} X^*_{-\tau}\omega \wedge *X^*_{-\tau}\eta = \int_\Omega \omega \wedge *\eta + R(\boldsymbol{\beta}, \tau)\int_\Omega \omega \wedge *\eta,$$

with $|R(\boldsymbol{\beta}, \tau)| \le C(\boldsymbol{\beta})\tau$ independent of ω and η.

By density of $\mathcal{F}^p(\Omega)$ in $L^2(\Omega)$ it is enough to prove the assertions for smooth $\eta, \omega \in \mathcal{F}^p(\Omega)$. In what follows $S(p, n)$ is the set of permutations σ of numbers $\{1, 2, \ldots, n\}$, such that $\sigma(1) < \cdots < \sigma(p)$ and $\sigma(p + 1) < \cdots < \sigma(n)$. By multi-linearity we have for orthonormal vector fields $\boldsymbol{e}_1, \ldots, \boldsymbol{e}_n$ and $\sigma \in S(p, n)$, $\gamma \in \mathcal{F}^p(\Omega)$ and $x \in \Omega$ [35, p. 610]:

$$\begin{aligned}&\left(X^*_\tau\gamma\right)_x(\boldsymbol{e}_{\sigma(1)}, \ldots, \boldsymbol{e}_{\sigma(p)})\\ &\quad= \sum_{\sigma' \in S(j,n)} \det\left(\left(DX_\tau(x)\right)_{\sigma',\sigma}\right)\gamma_{X_\tau(x)}(\boldsymbol{e}_{\sigma'(1)}, \ldots, \boldsymbol{e}_{\sigma'(p)}),\end{aligned} \tag{4.14}$$

where the quantities $\det((DX_\tau(x))_{\sigma',\sigma})$ are known as the p-minors of the differential $DX_\tau(x)$ with respect to $\boldsymbol{e}_1, \ldots, \boldsymbol{e}_n$, i.e. the determinants of those submatrices of $DX_\tau(x)$, that contain the rows σ' and columns σ. By the definition of the inner product of differential forms we have

$$\int_{X_\tau(\Omega)} X^*_{-\tau}\omega \wedge *X^*_{-\tau}\eta = \int_{X_\tau(\Omega)} \left\langle X^*_{-\tau}\omega, X^*_{-\tau}\eta\right\rangle \mathrm{vol},$$

where vol is the unique volume form on Ω and $\langle\cdot,\cdot\rangle$ [36, Definition 1.2.2b)] is the scalar product of alternating linear forms, which reads

$$\langle \omega_x, \eta_x \rangle := \sum_{\sigma \in S(p,n)} \omega_x(\boldsymbol{e}_{\sigma(1)}, \ldots, \boldsymbol{e}_{\sigma(n)}) \eta_x(\boldsymbol{e}_{\sigma(1)}, \ldots, \boldsymbol{e}_{\sigma(n)}).$$

Hence, (4.14) and the change of variable formula yield

$$\int_{X_\tau(\Omega)} X_{-\tau}^* \omega \wedge * X_{-\tau}^* \eta = \int_\Omega \det(DX_\tau) \big\langle \boldsymbol{M}_p(DX_\tau)\omega, \boldsymbol{M}_p(DX_\tau)\eta \big\rangle \,\mathrm{vol}, \tag{4.15}$$

with

$$\begin{aligned} &\big(\boldsymbol{M}_p\big(DX_\tau(x)\big)\gamma_x\big)(\boldsymbol{e}_{\sigma(1)}, \ldots, \boldsymbol{e}_{\sigma(j)}) \\ &\quad := \sum_{\sigma' \in S(p,n)} \det\big(\big(DX_\tau(x)\big)_{\sigma',\sigma}\big)\gamma_x(\boldsymbol{e}_{\sigma'(1)}, \ldots, \boldsymbol{e}_{\sigma'(p)}). \end{aligned} \tag{4.16}$$

Now, Taylor expansion of $\int_{X_\tau(\Omega)} X_{-\tau}^* \omega \wedge * X_{-\tau}^* \eta$ in τ around $\tau = 0$ boils down to Taylor expansion of the multiplication coefficients $\det((DX_\tau(x))_{\sigma',\sigma})$. From the Taylor expansion of $DX_\tau(x)$, $DX_\tau(x) = I_n + \int_0^\tau D\boldsymbol{\beta}(X_s(x))DX_s(x)ds$ and the Taylor expansion of det(), $\det(\boldsymbol{A}(\tau)) = \det(\boldsymbol{A}(0)) + \int_0^\tau \mathrm{trace}(\mathrm{Adj}(\boldsymbol{A}(s))\frac{d\boldsymbol{A}}{ds})ds$ and (4.16) we infer

$$\begin{aligned} &\big(\boldsymbol{M}_p\big(DX_\tau(x)\big)\gamma_x\big)(\boldsymbol{e}_{\sigma(1)}, \ldots, \boldsymbol{e}_{\sigma(p)}) \\ &\quad = \sum_{\sigma' \in S(p,n)} \det\big((I_n)_{\sigma',\sigma}\big)\gamma_x(\boldsymbol{e}_{\sigma'(1)}, \ldots, \boldsymbol{e}_{\sigma'(p)}) \\ &\qquad + \sum_{\sigma' \in S(p,n)} R_{\sigma',\sigma}(D\boldsymbol{\beta}, \tau)\gamma_x(\boldsymbol{e}_{\sigma'(1)}, \ldots, \boldsymbol{e}_{\sigma'(p)}), \end{aligned} \tag{4.17}$$

with Adj and trace the adjugate and trace operator for matrices, the unit matrix $I_n \in \mathbb{R}^{n\times n}$, and $|R_{\sigma',\sigma}(D\boldsymbol{\beta}, \tau)| \le \tau C_{\sigma',\sigma}(D\boldsymbol{\beta})$, $C_{\sigma',\sigma}$ independent of τ. Combining (4.15) and (4.17) yields the assertion. □

Remark 4.3 For $\tau = T$ the semi-Lagrangian schemes seem to provide $\omega(T)$ in one step. This is true, but irrelevant, because we are studying semi-Lagrangian methods as building blocks for the discretization of the advection-diffusion problem (1.2), see [20]. Unduly large timesteps will make the scheme miss the diffusion completely. Therefore, τ has to be linked to the spatial meshwidth h.

Remark 4.4 According to Theorem 4.1, for the convergence of the semi-Lagrangian schemes it suffices to link τ to h so that $\tau \to 0$ as $h \to 0$. Moreover, if we chose $\tau = const.\ h^\delta$, with δ arbitrary small then an almost optimal rate of convergence follows from the error bound in Theorem 4.1. For practical semi-Lagrangian methods, in particular when additionally diffusion is to be treated by some splitting scheme, a timestep size $\tau = O(h)$ would be desirable. In that case the estimates in Theorem 4.1 are not optimal. In particular convergence for $r = 0$ is not implied.

The following theorem provides a refined estimate for the Galerkin projection scheme (4.8), which will partly remedy the shortcomings of Theorem 4.1 pointed out in the previous Remark 4.4. It generalizes a result of [25, p. 52] to advection problems for differential forms with non-constant velocity and non-homogeneous right-hand side. In particular, even if $\tau = O(h)$, L^2-convergence of the semi-Lagrangian scheme will follow from mere first order best approximation estimates for the trial spaces $\mathcal{W}^p(\Omega_h)$.

Theorem 4.2 *Let $\omega \in H^s(\Omega)$ and $\omega_h \in \mathcal{W}^p(\Omega_h)$ be the solutions of (1.4) and (4.8). Further assume that*

$$\left\| \Pi_h^p \omega - \omega \right\|_0 \leq C_p h^{\min(s,r+1)} \|\omega\|_s \quad \forall \omega \in H^s(\Omega). \tag{4.18}$$

If Assumption (A.1) holds, then

$$\max_{0\leq i\leq N} \left\| \omega^i - \omega_h^i \right\|_0 \leq C h^{\min(s,r+1)} \left(\frac{1}{\sqrt{\tau}} + 1 \right) \max_{0\leq n\leq N} \left\| \omega^n \right\|_s, \tag{4.19}$$

where $\omega^i = \omega(i\tau)$ and $C > 0$ depends only on C_p from (4.18) and $\boldsymbol{\beta}$.

Proof The solution formula (2.10), the definition (4.8) of ω_h^{i+1} and the Pythagorean theorem yield the following *recursive estimate* for the norm of the error $e^{i+1} := \omega^{i+1} - \omega_h^{i+1}$:

$$\begin{aligned} \left\| e^i \right\|_0^2 &= \left\| \omega^i - \Pi_h^p \omega^i + \Pi_h^p \omega^i - \omega_h^i \right\|_0^2 \\ &= \left\| \omega^i - \Pi_h^p \omega^i + \Pi_h^p X_{-\tau}^* \left(\omega^{i-1} - \omega_h^{i-1} \right) \right\|_0^2 \\ &= \left\| \omega^i - \Pi_h^p \omega^i \right\|_0^2 + \left\| \Pi_h^p X_{-\tau}^* \left(\omega^{i-1} - \omega_h^{i-1} \right) \right\|_0^2. \end{aligned}$$

Since we assume vanishing normal component of $\boldsymbol{\beta}$ on the boundary of Ω (Assumption A.1), we can use Lemma 4.1 together with the L^2-stability of the orthogonal projection Π_h^p to obtain

$$\left\| e^i \right\|_0^2 \leq \xi^i + (1 + C_e \tau) \left\| e^{i-1} \right\|_0^2,$$

with the spatial projection errors $\xi^i := \|\omega^i - \Pi_h^p \omega^i\|_0^2$. A discrete Gronwall-like inequality and the approximation assumption (4.18) yield with $m := \min(s, r+1)$

$$\begin{aligned} \left\| e^i \right\|_0^2 &\leq \frac{\exp(C_e \tau i) - 1}{C_e \tau} \max_{0\leq n<i} \xi^n + \left\| \xi^i \right\|_0^2 \\ &\leq C_p \frac{\exp(C_e \tau i) - 1}{C_e \tau} h^m \max_{0\leq n<i} \left\| \omega^n \right\|_{s,q}^2 + C_p h^m \left\| \omega^i \right\|_s^2, \end{aligned} \tag{4.20}$$

and the assertion follows. □

5 Fully discrete semi-Lagrangian schemes

An actual implementation of schemes (4.8) and (4.6) requires further approximations. This needs to be done very carefully in order to preserve the favorable stability properties of Lagrangian schemes established in Theorem 4.1. A shape-regular family of simplicial meshes $(\Omega_h)_h$ with meshwidth h is taken for granted.

(i) *Approximate flow map*. First we would like to introduce approximations $\bar{X}_\tau$ of the flow map X_τ that depend on both Ω_h and the timestep τ. We require consistency in the following sense:

- $\bar{X}_\tau : \Omega \mapsto \Omega$ is Ω_h-piecewise smooth,
- there are $k, l \geq 1$ such that for $h \to 0$ and $\tau \to 0$

$$\|X_\tau - \bar{X}_\tau\|_{\mathbf{W}^{0,\infty}} \leq O\big(h^{k+1}\tau + \tau^l\big) \quad \text{and} \quad |X_\tau - \bar{X}_\tau|_{\mathbf{W}^{1,\infty}} \leq O\big(h^k\tau + \tau^l\big). \tag{5.1}$$

A simple construction of approximate flow maps relies on the nodal basis functions $(\lambda_i)_i$ spanning the space of continuous piecewise polynomial Lagrangian finite element functions of degree k. The degrees of freedom associated to these basis functions are point evaluations at particular nodal points $(\boldsymbol{a}_i)_i$ defined by affine coordinates inside the simplices of the mesh. Then we define

$$\bar{X}_\tau(\boldsymbol{x}) := \sum_i \bar{X}_{\tau,i}\lambda_i(\boldsymbol{x}), \tag{5.2}$$

where the coefficients $\bar{X}_{\tau,i}$ are approximations to the trajectories $X_\tau(\boldsymbol{a}_i)$ of the interpolation points $\boldsymbol{a}_i$ of order l:

$$\big\|X_\tau(\boldsymbol{a}_i) - \bar{X}_{\tau,i}\big\| \leq C\tau^l \quad \text{for } \tau \to 0,\ \forall i, \tag{5.3}$$

uniformly in h for some vector norm $\|\cdot\|$, see Fig. 1 for an illustration.

This approximation is consistent by construction. The error $|X_\tau - \bar{X}_\tau|_{\mathbf{W}^{s,\infty}}$, $s = 0, 1$, splits into an error originating from approximations of the trajectories of the degrees of freedom, which is assumed to be of order $O(\tau^l)$, and an error due to interpolation in Lagrangian finite element spaces. The bound on the interpolation error follows from standard interpolation estimates for Lagrangian finite elements [8, Sect. 3.1]. If Π_h denotes the interpolation operator $\Pi_h f := \sum_i f(\boldsymbol{a}_i)\lambda_i$, $f \in C^0(\overline{\Omega})$, and $\boldsymbol{\beta} \in \mathbf{W}^{k+1,\infty}(\Omega)$ we can estimate

$$\begin{aligned} |X_\tau - \Pi_h X_\tau|_{\mathbf{W}^{s,\infty}} &= \big|X_\tau - \mathrm{id} - \Pi_h(X_\tau - \mathrm{id})\big|_{\mathbf{W}^{s,\infty}} \\ &\leq Ch^{k+1-s}|X_\tau - \mathrm{id}\,|_{\mathbf{W}^{k+1,\infty}} \leq Ch^{k+1-s}\tau\|\boldsymbol{\beta}\|_{\mathbf{W}^{k+1,\infty}}, \end{aligned}$$

where the last inequality follows from (2.1) and the constants depend neither on h nor τ.

(ii) *Approximation of the source*. We have to approximate the time integration of the right-hand side in (4.6) and (4.8). Since φ does not depend on ω, it is reasonable to chose some quadrature method for the approximation $Q(\varphi, t, t+\tau) \approx$

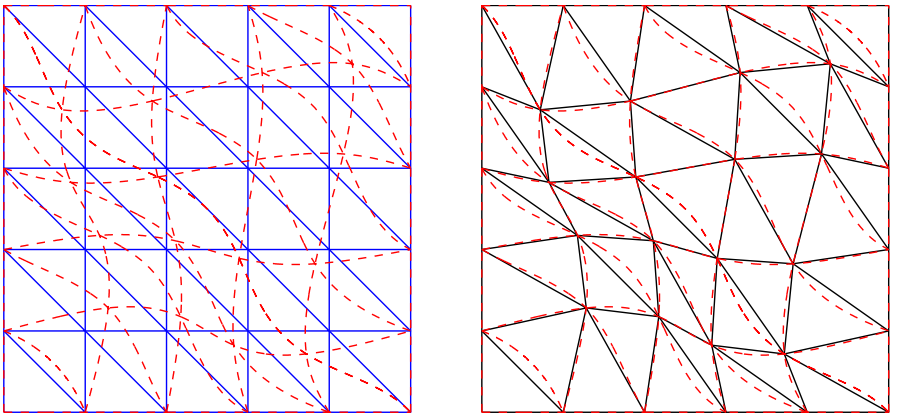

Fig. 1 Illustration of the approximation of the flow map X_τ. *Left*: The fixed mesh Ω_h (*solid lines*) and its image $X_\tau(\Omega_h)$ (*dashed lines*) under the exact flow. For smooth $\boldsymbol{\beta}$ $X_\tau(\Omega_h)$ consists of non-polynomial curved polygons. *Right*: A low order consistent approximation $\bar{X}_\tau(\Omega_h)$ (*solid lines*) of $X_\tau(\Omega_h)$ (*dashed lines*). Here we used linear Lagrangian elements and exact trajectories for the vertices, hence $\bar{X}_\tau(\Omega_h)$ has again straight edges and the vertices of $X_\tau(\Omega_h)$ and $\bar{X}_\tau(\Omega_h)$ coincide

$\int_t^{t+\tau} \varphi(s)ds$ which satisfies

$$\left| \int_t^{t+\tau} \varphi(s)ds - Q(\varphi, t, \tau) \right| \leq C\tau^m \max_{t\leq s\leq t+\tau} \left| \frac{d^m}{dt^m}\varphi(s) \right|, \quad m \geq 2. \tag{5.4}$$

Now we are in a position to formulate fully discrete semi-Lagrangian timestepping schemes.

(1) *Fully discrete Galerkin projection scheme*. Find $\omega_h^i \in \mathcal{W}^p(\Omega_h)$, $i = 0, \ldots, N$, such that for all $\eta_h \in \mathcal{W}^p(\Omega_h)$:

$$\begin{aligned} \left(\omega_h^0, \eta_h\right)_\Omega &= (\omega_0, \eta_h)_\Omega; \\ \left(\omega_h^{i+1}, \eta_h\right)_\Omega &= \left(\bar{X}_{-\tau}^* \omega_h^i, \eta_h\right)_\Omega + \left(Q\left(\bar{X}_{s-t_{i+1}}^* \widetilde{\varphi}(s), t_i, t_{i+1}\right), \eta_h\right)_\Omega. \end{aligned} \tag{5.5}$$

For $p = 0$ and continuous piecewise linear approximation spaces (5.5) is exactly the scheme in [32].

(2) *Fully discrete interpolation scheme*. Find $\omega_h^i \in \mathcal{W}^p(\Omega_h)$, $i = 0, \ldots, N$, such that:

$$\begin{aligned} \omega_h^0 &= I_h^p \omega_0; \\ \omega_h^{i+1} &= I_h^p \bar{X}_{-\tau}^* \omega_h^i + I_h^p Q\left(\bar{X}_{s-t_{i+1}}^* \widetilde{\varphi}(s), t_i, t_{i+1}\right). \end{aligned} \tag{5.6}$$

Owing to the approximation (5.2) of the flow map, the pullbacks are still piecewise polynomial. Hence, the right-hand sides in (5.6) and (5.5) can be computed exactly. For instance, for the Galerkin projection scheme (5.5) this can be done after

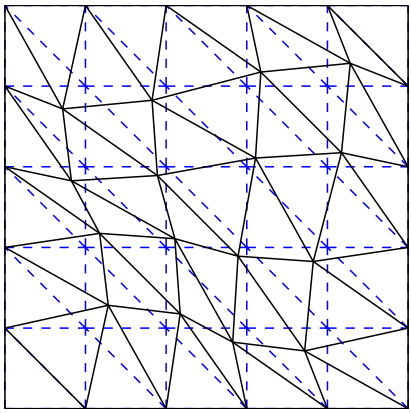

Fig. 2 The inner products on the right-hand side of the Galerkin projection scheme (5.5) pair finite element functions defined on two different meshes, namely the fixed mesh (*dashed lines*) and the approximated transported mesh (*solid lines*). Since in both meshes the facets are polynomial, we can algorithmically determine a partitioning of Ω such that all appearing finite element functions are smooth on each part. The finite element functions and the pullbacks are polynomials, hence the inner products can be computed exactly

the intersections of all elements K of the mesh Ω_h with all elements $\bar{X}_\tau(K')$ of the transported mesh $\bar{X}_\tau(\Omega_h)$ have been found (see Fig. 2 for illustration).

At a first glance this seems to be very expensive. Nevertheless we contend that at least for the case of low order approximations ($k = 0$) such schemes provide competitive methods.

The interpolation schemes (5.6) are cheaper in certain cases. In particular, in the case of lowest order approximation and $p < n$ the degrees of freedom are simple facet integrals and we need to find only intersections of transported p-dimensional facets with elements K of mesh Ω_h. In addition, the interpolation schemes give entirely explicit schemes, whereas for the Galerkin projection schemes we have to solve a linear system in each timestep, unless clever mass lumping is employed, which might not be available for higher polynomial degree and $0 < p < n$. Algorithmic details for interpolation schemes are discussed in [18, Sect. 3].

Remark 5.1 Inspired by standard finite element techniques one could be tempted to split the inner product $(\bar{X}^*_{-\tau}\omega_h, \eta_h)_\Omega$ into a sum of integrals over elements of Ω_h and apply some quadrature rule there. We dub this scheme the *quadrature-based scheme*:

Find $\omega_h^i \in \mathcal{W}^p(\Omega_h)$, $i = 0, \dots, N$, such that for all $\eta_h \in \mathcal{W}^p(\Omega_h)$:

$$\begin{aligned} \big(\omega_h^0, \eta_h\big)_{\Omega,h} &= (\omega_0, \eta_h)_{\Omega,h}; \\ \big(\omega_h^{i+1}, \eta_h\big)_{\Omega,h} &= \big(\bar{X}^*_{-\tau}\omega_h^i, \eta_h\big)_{\Omega,h} + \big(Q\big(\bar{X}_{s-t_{i+1}}\widetilde{\varphi}(s), t_i, t_{i+1}\big), \eta_h\big)_{\Omega,h}, \end{aligned} \tag{5.7}$$

with

$$(\omega, \eta)_{\Omega,h} = \sum_{K\in\Omega_h} \sum_i w_{i,K}\,\omega(x_{i,K}) \wedge *\eta(x_{i,K}), \tag{5.8}$$

for suitable quadrature points $(x_{i,K})_i \in K$ and quadrature weights $(w_{i,K})_i$. Compared to the projection scheme this reduces the computational cost, since only the trajectories for the quadrature points need to be computed. However, for $p > 0$ this scheme is dubious since we apply quadrature on domains with discontinuous integrands. Our experiments in the next section (see Example 2) show that these doubts are justified. We also refer to the article [27] that investigated the case $p = 0$ on quadrilateral meshes. It was shown that Semi-Lagrangian schemes with quadrature can be unconditional unstable. In contrast, the purely spectral semi-Lagrangian methods in [38] and [3] with globally smooth basis functions retain the unconditional stability even for the case of quadrature.

In analogy to Theorem 4.2 we can prove convergence for the solutions of the fully discrete Galerkin projection scheme (5.5). To begin with, we show that for sufficiently smooth velocity $\boldsymbol{\beta}$ our consistent approximations of the flow map fulfill

$$\left\| X^*_{-\tau}\omega - \bar{X}^*_{-\tau}\omega \right\|_0 \leq C_f \left(h^k \tau + \tau^l\right) \|\omega\|_1, \tag{5.9}$$

for $C_f = C_f(\boldsymbol{\beta}, D\boldsymbol{\beta}) > 0$ independent of h and τ.

Lemma 5.1 *Assume that the velocity field $\boldsymbol{\beta}$ satisfies $\|\boldsymbol{\beta}\|_{\mathbf{W}^{k+1,\infty}(\Omega)} \leq \infty$. Then a consistent approximation of the flow map according to (5.2) fulfills (5.9).*

Proof The proof uses similar arguments as the proof of Lemma 4.1. With the notation introduced there, we have in particular

$$\left\| X^*_{-\tau}\omega - \bar{X}^*_{-\tau}\omega \right\|_0^2 = \int_\Omega \left\langle X^*_{-\tau}\omega - \bar{X}^*_{-\tau}\omega,\, X^*_{-\tau}\omega - \bar{X}^*_{-\tau}\omega \right\rangle \mathrm{vol}.$$

For fixed $x \in \Omega$ and τ we introduce the abbreviations $\omega_x(\boldsymbol{e}_\sigma) := \omega_x(\boldsymbol{e}_{\sigma(1)}, \ldots, \boldsymbol{e}_{\sigma(p)})$, $\omega_X := \omega_{X_{-\tau}(x)}$ and $DX := DX_{-\tau}(x)$. Then we find

$$\left(X^*_{-\tau}\omega\right)_x(\boldsymbol{e}_\sigma) = \boldsymbol{M}_p(DX)\omega_X(\boldsymbol{e}_\sigma) \quad \text{and} \quad \left(\bar{X}^*_{-\tau}\omega\right)_x(\boldsymbol{e}_\sigma) = \boldsymbol{M}_p(D\bar{X})\omega_{\bar{X}}(\boldsymbol{e}_\sigma),$$

where $\boldsymbol{M}_p(\cdot)$ is the operator introduced in (4.16). Together this yields

$$\begin{aligned}\left(X^*_{-\tau}\omega - \bar{X}^*_{-\tau}\omega\right)_x(\boldsymbol{e}_\sigma) = &\left(\boldsymbol{M}_p(DX)\omega_X - \boldsymbol{M}_p(D\bar{X})\omega_X\right)(\boldsymbol{e}_\sigma) \\ &+ \left(\boldsymbol{M}_p(D\bar{X})\omega_X - \boldsymbol{M}_p(D\bar{X})\omega_{\bar{X}}\right)(\boldsymbol{e}_\sigma).\end{aligned}$$

For each σ' we have that $\omega_X(\boldsymbol{e}_{\sigma'})$ is a function of X, i.e. for smooth differential forms Taylor expansion yields

$$\omega_X(\boldsymbol{e}_{\sigma'}) = \omega_{\bar{X}}(\boldsymbol{e}_{\sigma'}) + (X - \bar{X})\partial_x \omega_x(\boldsymbol{e}_{\sigma'})_{|x = X + s(X - \bar{X})},$$

for some s with $0 \leq s \leq 1$. We find

$$\left\| X^*_{-\tau}\omega - \bar{X}^*_{-\tau}\omega \right\|_0^2 \leq a_1 + a_2,$$

with

$$a_1 = \sup_x K_1\big(DX_{-\tau}(x) - D\bar{X}_{-\tau}(x)\big)\|\omega\|_0^2$$

and

$$a_2 = \sup_x K_2\big(X_{-\tau}(x) - \bar{X}_{-\tau}(x)\big)|\omega|_1^2,$$

where $K_1(\cdot)$ and $K_2(\cdot)$ are smooth functions. We get the bound

$$\big\|X_{-\tau}^*\omega - \bar{X}_{-\tau}^*\omega\big\|_0^2 \le C|X_{-\tau} - \bar{X}_{-\tau}|_{\mathbf{W}^{1,\infty}}^2\|\omega\|_0^2 + C\|X_{-\tau} - \bar{X}_{-\tau}\|_{\mathbf{W}^{0,\infty}}^2|\omega|_1^2$$

and the assertion follows by (5.1). □

Next we prove a counterpart of Lemma 4.1, i.e. stability of $\|\bar{X}_{-\tau}^*\omega\|_0$.

Lemma 5.2 *Let $\bar{X}_\tau$ be the approximation of the flow X_τ defined in (5.2). If $\boldsymbol{\beta} \in \mathbf{W}^{k+1,\infty}(\Omega)$ and $\omega \in L^2(\Omega)$ is compactly supported in Ω, we can bound for sufficiently small τ*

$$\big\|\bar{X}_{-\tau}^*\omega\big\|_0^2 \le (1 + \bar{C}_e\tau)\|\omega\|_0^2, \tag{5.10}$$

with $\bar{C}_e = \bar{C}_e(\boldsymbol{\beta}, h, \tau) = C_e + C(\boldsymbol{\beta})(h^k + \tau^{l-1}) > 0$ independent of ω.

Proof The assertion follows by the same arguments as the proof of Lemma 4.1 due to

$$\begin{aligned}\|D\bar{X}_{-\tau}\|_{\mathbf{W}^{0,\infty}} &\le \|DX_{-\tau}\|_{\mathbf{W}^{0,\infty}} + \|D\bar{X}_{-\tau} - DX_{-\tau}\|_{\mathbf{W}^{0,\infty}}\\ &\le 1 + C_e\tau + C(\beta)\big(h^k\tau + \tau^l\big),\end{aligned}$$

by smoothness of $\boldsymbol{\beta}$ and the bounds (5.1) on the approximate flow map. □

This lemma paves the way for extending Theorem 4.2 to the fully discrete projection scheme.

Theorem 5.1 *Let the assumptions of Theorem 4.2 and Lemma 5.2 hold, and $\omega_h \in \mathcal{W}^p(\Omega_h)$ be the solution of (5.5) with $\bar{X}_\tau$ given by (5.2). Further, we assume that the approximation of the time integration of the source term in (5.6) is of order m according to (5.4).*

Then, for h and τ sufficiently small,

$$\begin{aligned}\max_{0\le i\le N}\big\|\omega^i - \omega_h^i\big\|_0 \le& C\left(\frac{1}{\sqrt{\tau}} + 1\right)\big(h^{\min(s,r+1)} + \tau h^k + \tau^l\big)\max_{0\le n\le N}\big\|\omega^n\big\|_s\\ &+ C\left(\frac{1}{\sqrt{\tau}} + 1\right)\big(\tau^{m-1} + \tau h^k + \tau^l\big)C(\widetilde{\varphi}),\end{aligned}$$

where $\omega^i = \omega(i\tau)$ and C independent of h and τ.

Proof The proof is similar to that of Theorem 4.2. The additional approximations of the flow and the source term spawn consistency error terms in the error recursion. First, we introduce an approximate solution $(\bar{\omega}^i)_{i=0}^N$ taking into account the perturbation of the flow and quadrature for the right-hand side:

$$\begin{aligned} \bar{\omega}^0 &= \omega_0; \\ \bar{\omega}^{i+1} &= \bar{X}^*_{-\tau}\bar{\omega}^i + Q\big(\bar{X}^*_{s-t_{i+1}}\widetilde{\varphi}(s), t_i, t_{i+1}\big). \end{aligned} \tag{5.11}$$

Then we split the error $\|\omega^i - \omega_h^i\|_0$ as follows

$$\big\|\omega^i - \omega_h^i\big\|_0 \le \big\|\omega^i - \bar{\omega}^i\big\|_0 + \big\|\bar{\omega}^i - \omega_h^i\big\|_0 := \big\|\bar{e}^i\big\|_0 + \big\|e^i\big\|_0. \tag{5.12}$$

We find

$$\begin{aligned} \big\|\bar{e}^i\big\|_0 = \big\|\omega^i - \bar{\omega}^i\big\|_0 &\le \big\|X^*_{-\tau}\omega^{i-1} - \bar{X}^*_{-\tau}\bar{\omega}^{i-1}\big\|_0 \\ &\quad + \left\| \int_{t_{i-1}}^{t_i} X^*_{s-t_i}\widetilde{\varphi}(s)ds - Q\big(\bar{X}^*_{s-t_i}\widetilde{\varphi}(s), t_{i-1}, t_i\big)\right\|_0 \\ &:= E_1 + E_2. \end{aligned}$$

For the first error term E_1 we deduce from Lemma 5.2, bound (5.9) and $l \ge 1$:

$$\begin{aligned} E_1 &\le \big\|X^*_{-\tau}\omega^{i-1} - \bar{X}^*_{-\tau}\bar{\omega}^{i-1}\big\|_0 \\ &\le \big\|\bar{X}^*_{-\tau}\omega^{i-1} - \bar{X}^*_{-\tau}\bar{\omega}^{i-1}\big\|_0 + \big\|\big(X^*_{-\tau} - \bar{X}^*_{-\tau}\big)\omega^{i-1}\big\|_0 \\ &\le (1 + \bar{C}_e\tau)\big\|\omega^{i-1} - \bar{\omega}^{i-1}\big\|_0 + C_f\big(h^k\tau + \tau^l\big)\big\|\omega^{i-1}\big\|_1. \end{aligned}$$

Hence we get the error recursion

$$\begin{aligned} \big\|\bar{e}^i\big\|_0 &\le (1 + \bar{C}_e\tau)\big\|\bar{e}^{i-1}\big\|_0 + C_f\big(h^k\tau + \tau^l\big)\big\|\omega^{i-1}\big\|_1 + E_2 \\ &\le (1 + \bar{C}_e\tau)^i\big\|\bar{e}^0\big\|_0 + C_f\big(h^k\tau + \tau^l\big)\sum_{n=0}^{i-1}(1 + \bar{C}_e\tau)^{i-n}\big\|\omega^n\big\|_1 + iE_2 \\ &\le C_f\big(h^k\tau + \tau^l\big)\max_{0\le n\le N}\big\|\omega^n\big\|_1\sum_{n=0}^{i-1}(1 + \bar{C}_e\tau)^n + \frac{T}{\tau}E_2 \\ &\le C_f\big(h^k\tau + \tau^l\big)\max_{0\le n\le N}\big\|\omega^n\big\|_1\frac{\exp(\bar{C}_eT) - 1}{\bar{C}_e\tau} + \frac{T}{\tau}E_2. \end{aligned} \tag{5.13}$$

For the term E_2 we get from bound (5.9) and the approximation of the source:

$$\begin{aligned} E_2 &\le \left\| \int_{t_{i-1}}^{t_i} X^*_{s-t_i}\widetilde{\varphi}(s)\,ds - Q\big(\bar{X}^*_{s-t_i}\widetilde{\varphi}(s), t_{i-1}, t_i\big)\right\|_0 \\ &\le \left\| \int_{t_{i-1}}^{t_i} \bar{X}^*_{s-t_i}\widetilde{\varphi}(s)\,ds - Q\big(\bar{X}^*_{s-t_i}\widetilde{\varphi}(s), t_{i-1}, t_i\big)\right\|_0 \end{aligned}$$

$$+ \left\| \int_{t_{i-1}}^{t_i} \bar{X}^*_{s-t_i} \widetilde{\varphi}(s)\, ds - \int_{t_{i-1}}^{t_i} X^*_{s-t_i} \widetilde{\varphi}(s)\, ds \right\|_0$$
$$\leq C_1(\widetilde{\varphi})\tau^m + C_2(\widetilde{\varphi})\big(h^k \tau^2 + \tau^{l+1}\big), \tag{5.14}$$

with $C_1(\widetilde{\varphi})$ and $C_2(\widetilde{\varphi})$ independent of h and τ. For the second error term $\|e^i\|_0$ we obtain the bound

$$\left\|e^i\right\|_0 \leq K\left(\frac{1}{\sqrt{\tau}} + 1\right) \max_{0\leq n\leq N} \big(h^{\min(s,r+1)} \left\|\omega^n\right\|_s + \left\|\bar{e}^n\right\|_0\big), \tag{5.15}$$

for some $K = K(\bar{C}_e) > 0$, that is bounded for $h, \tau \to 0$. The proof is analogue to the proof of Theorem 4.2 where here the fully discrete scheme (5.5) is treated as an exact Galerkin projection scheme for (5.11). We combine (5.12) with (5.13) and (5.15) and obtain the assertion. □

6 Numerical experiments: advection of 1-forms in $\mathbb{R}^2$

In this section we and study the performance of both the fully discrete semi-Lagrangian interpolation (5.6) and the fully discrete semi-Lagrangian Galerkin projection scheme (5.5) for the advection problem (1.4) for time-dependent 1-forms $\omega \in C^1([0,T], L^{2,1}(\Omega))$, $\Omega \subset \mathbb{R}^2$, with compactly supported initial data ω_0. In vector proxy notion with $\mathbf{u} := \text{v.p.}(\omega)$ this reads

$$\begin{aligned} \partial_t \mathbf{u} + \mathbf{grad}(\boldsymbol{\beta} \cdot \mathbf{u}) + \boldsymbol{R}^T \mathsf{div}(\boldsymbol{R}\mathbf{u})\boldsymbol{\beta} = \mathbf{f} \quad &\text{in } \Omega, \\ \mathbf{u}(0) = \mathbf{u}_0 \quad &\text{in } \Omega, \end{aligned} \tag{6.1}$$

with $\mathbf{R} = \left(\begin{smallmatrix} 0 & 1 \\ -1 & 0 \end{smallmatrix}\right)$. We approximate ω by lowest order discrete 1-forms $\omega_h \in \mathcal{W}_0^1(\Omega_h)$ on a triangular mesh Ω_h. The discrete space $\mathcal{W}_0^1(\Omega_h)$ consists of tangentially continuous, piecewise polynomial functions, with piecewise constant exterior derivatives ("edge elements"). The basis functions are associated with the edges of the mesh and the degrees of freedom are line integrals on edges.

Further, we use continuous piecewise linear Lagrangian finite elements to approximate the flow map (5.2). If not stated differently, we use explicit Euler timesteps to determine the flow of the vertices. Thus, the transported mesh $\bar{X}_\tau(\Omega_h)$ is again a mesh with straight edges. The inner products for both, the Galerkin projection scheme and the interpolation scheme, are calculated exactly. The right-hand sides are evaluated by means of one-point quadrature in time, using the endpoint of the integration interval (5.4). In this setting the various orders of consistency entering the estimates of Theorem 5.1 are $r = 0$, $k = 1$, $l = 2$, $m = 1$.

In the following experiments we link the timestep size τ to the meshwidth h by the relationship

$$\tau = \gamma \frac{h}{\|\boldsymbol{\beta}\|_{\mathbf{W}^{0,\infty}(\Omega)}}, \tag{6.2}$$

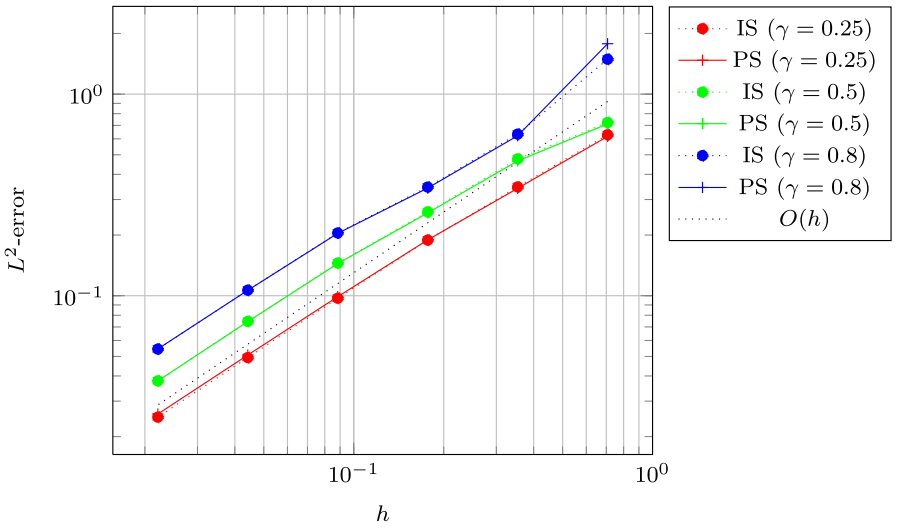

Fig. 3 Experiment 1: Convergence rates of L^2-error at $t = 0.4$ for the interpolation scheme (IS) and the Galerkin projection scheme (PS) on time interval $[0, 0.4]$ for $\gamma = 0.25$, $\gamma = 0.5$ and $\gamma = 0.8$ (Color figure online)

where $\gamma > 0$ is some constant. In most cases, we will choose $\gamma \approx 1$, which is advisable for the full advection-diffusion problem in a setting with (locally) significant diffusion. Remember that it is this class of problems that we aim to design methods for. Nevertheless, for the sake of brevity and clarity, we do not treat diffusion terms here.

6.1 Experiment 1: generic right-hand side

In (6.1), we consider $\Omega = (-1, 1)^2$ and choose the velocity

$$\boldsymbol{\beta} = \left(1 - x_1^2\right)\left(1 - x_2^2\right)\begin{pmatrix} 0.66 \\ 1 \end{pmatrix}.$$

The data $\mathbf{u}_0$ and $\mathbf{f}$ are chosen such that

$$\boldsymbol{u}(x, t) = \cos(2\pi t)\begin{pmatrix} \sin(\pi x_1)\sin(\pi x_2) \\ (1 - x_1^2)(1 - x_2^2) \end{pmatrix}$$

is the solution. With this choice we encounter a non-zero right-hand side in (6.1).

In Fig. 3 we monitor convergence of semi-Lagrangian schemes for different values of γ. Strikingly, in this example the discretization errors of the interpolation scheme and the Galerkin projection scheme almost agree. We clearly observe $O(h)$-convergence of the $L^2(\Omega)$-error for the projection scheme, much faster than a decay of the error like $O(h^{\frac{1}{2}})$ predicted by Theorem 5.1. Nor does theory provide an explanation of the perfect first order convergence displayed by the interpolation scheme.

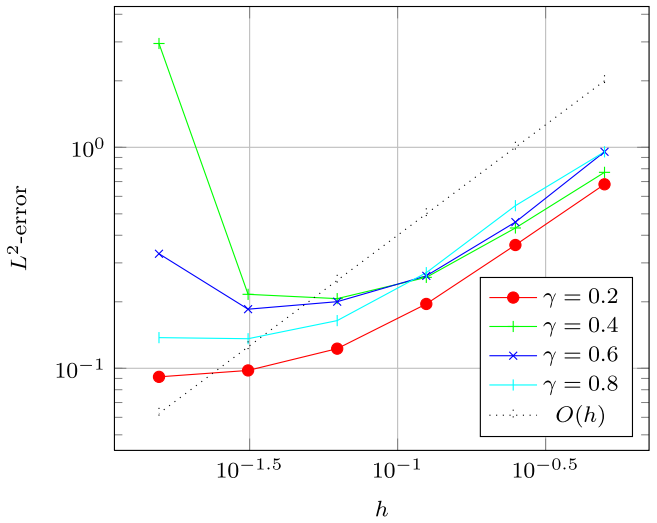

Fig. 4 Experiment 2: Convergence rate of the L^2-error at $t = 0.4$ for a Galerkin projection scheme with low order quadrature on the time interval $[0, 0.4]$ and $\gamma = 0.2$, $\gamma = 0.4$, $\gamma = 0.6$ and $\gamma = 0.8$ (Color figure online)

6.2 Experiment 2: failure of quadrature based scheme

The drawback of the Galerkin projection scheme obviously is the requirement to calculate the inner products $(\bar{X}^*_{-\tau}\omega_h, \eta_h)_\Omega$ exactly. A cheaper option is the quadrature-based scheme introduced in Remark 5.1.

We consider the same data for Problem (6.1) as in Experiment 1. Figure 4 shows the convergence rate of a quadrature-based scheme built on the barycenters as quadrature points. Only for a few initial refinement steps there is some sort of convergence, breaking down when we refine further. As in the scalar case $p = 0$ discussed in [27] the scheme seems to lack of unconditional stability. Moreover, even stability does not seem to guarantee convergence (see Fig. 5). This result is as expected since the quadrature-based scheme applies quadrature on domains with discontinuous integrands.

6.3 Experiment 3: vectorial rotating hump problem

Now we study the behaviour of the interpolation scheme (5.6) and the Galerkin projection scheme (5.5) for the classical rotating hump problem, cf. [5, 16, 24]: We consider problem (6.1) on a circular domain $\Omega := \{(x_1, x_2) : x_1^2 + x_2^2 < 1\}$ with source term $\boldsymbol{f} = 0$, velocity field

$$\boldsymbol{\beta}(\boldsymbol{x}) = \begin{pmatrix} x_2 \\ -x_1 \end{pmatrix}, \quad \boldsymbol{x} = (x_1, x_2) \in \Omega \tag{6.3}$$

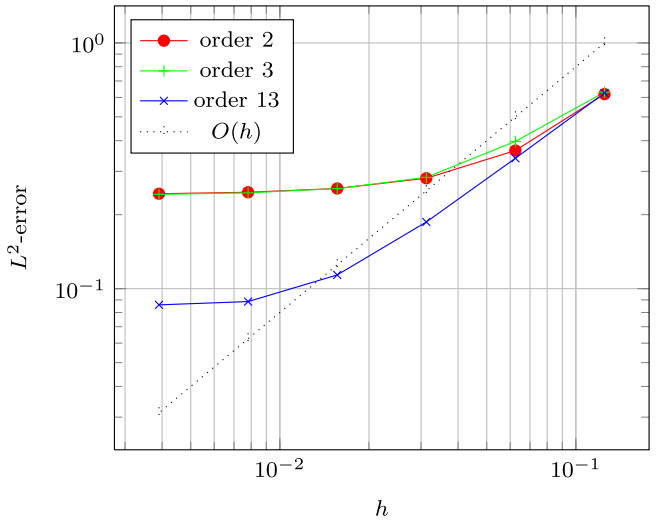

Fig. 5 Experiment 2: Convergence rate of the L^2-error at $t = 0.4$ for a Galerkin scheme with local quadrature rules of different orders on the time interval $[0, 0.4]$, $\gamma = 0.25$ (Color figure online)

and "smooth hump" initial data

$$\boldsymbol{u}_0(\boldsymbol{x}) := \begin{cases} \operatorname{grad} f(\boldsymbol{x}), & \text{for } \sqrt{x_1^2 + (x_2 - \frac{1}{4})^2} \le \frac{1}{2} \\ (0,0)^T, & \text{for } \sqrt{x_1^2 + (x_2 - \frac{1}{4})^2} > \frac{1}{2} \end{cases} \in C^2(\Omega), \tag{6.4}$$

with

$$f(\boldsymbol{x}) := \cos\left(\pi \sqrt{x_1^2 + \left(x_2 - \frac{1}{4}\right)^2}\right)^4. \tag{6.5}$$

The exact solution is

$$\boldsymbol{u}(t, \boldsymbol{x}) = \big(\boldsymbol{R}(t)\big)^{-1} \boldsymbol{u}_0\big(\boldsymbol{R}(t)\boldsymbol{x}\big), \quad \boldsymbol{R}(t) := \begin{pmatrix} \cos(t) & -\sin(t) \\ \sin(t) & \cos(t) \end{pmatrix}. \tag{6.6}$$

In order to study the impact of the approximation of the flow map, we use both (i) the explicit Euler method ($l = 2$ in (5.3)), and (ii) Heun's method ($l = 3$ in (5.3)) in order to determine the positions of the vertices of the advected mesh, cf. (5.2). Final time is $T = 2\pi$, that is, we track one full revolution. Tables 1, 2, 3, 4 list the L^2-errors of numerical solutions at $T = 2\pi$ for different meshwidths h and timestep sizes τ. As in Experiment 1, we witness conspicuous first order convergence. The numbers also convey the need for balancing h and τ, with higher order integration of trajectories allowing larger timesteps. First, for fixed meshwidth h we observe that the minimal error is not attained for the minimal timestep size, but for some intermediate values of τ.

Table 1 Experiment 3, rotating hump: L^2-error of the solution of the *interpolation scheme* (5.6) with explicit Euler method for different discretization parameters timestep τ (*rows*) and meshwidth h (*columns*)

$\tau \backslash h$	0.420	0.210	0.105	0.052	0.026
1.5707	1.86	1.89	1.86	1.88	2.33
0.7853	1.86	1.88	1.88	2.01	2.36
0.3926	1.84	1.82	1.80	2.01	2.32
0.1963	1.85	1.79	1.52	1.51	1.79
0.0997	1.85	1.80	1.54	1.05	1.02
0.0498	1.85	1.81	1.59	1.18	0.63
0.0249	1.85	1.81	1.61	1.26	0.79
0.0124	1.85	1.81	1.62	1.30	0.88
0.0062	1.85	1.81	1.63	1.31	0.92

Table 2 Experiment 3, rotating hump: L^2-error of the solution of the *interpolation scheme* (5.6) with Heun's method for different discretization parameters timestep τ (*rows*) and meshwidth h (*columns*)

$\tau \backslash h$	0.420	0.210	0.105	0.052	0.026
1.5707	1.85	1.86	1.91	2.12	2.47
0.7853	1.79	1.53	1.51	1.70	1.80
0.3926	1.83	1.56	0.99	0.55	0.50
0.1963	1.84	1.72	1.23	0.60	0.22
0.0997	1.84	1.77	1.49	0.85	0.33
0.0498	1.85	1.79	1.56	1.15	0.52
0.0249	1.85	1.80	1.59	1.24	0.79
0.0124	1.85	1.81	1.61	1.28	0.87
0.0062	1.85	1.81	1.62	1.31	0.92

Table 3 Experiment 3, rotating hump: L^2-error of the solution of the *Galerkin projection scheme* (5.5) with explicit Euler method for different discretization parameters timestep τ (*rows*) and meshwidth h (*columns*)

$\tau \backslash h$	0.420	0.210	0.105	0.052	0.026
1.5707	1.85	1.86	1.90	2.11	2.45
0.7853	1.85	1.85	1.87	2.02	2.32
0.3926	1.84	1.80	1.78	1.99	2.29
0.1963	1.84	1.79	1.57	1.49	1.75
0.0997	1.84	1.80	1.60	1.18	1.01
0.0498	1.85	1.81	1.64	1.31	0.75
0.0249	1.85	1.81	1.66	1.39	0.96
0.0124	1.85	1.82	1.68	1.40	1.01
0.0062	1.85	1.82	1.69	1.43	1.11

Second, when comparing the errors for the two integration schemes, we see that the minimal error for Heun's method is attained for larger values of τ than for the explicit Euler method. This reflects the higher order approximation properties of Heun's method, that appear explicitly in the estimate of Theorem 5.1 for the Galerkin projection scheme.

For our choice of data we find that the solution fulfills $\mathrm{div}\boldsymbol{Ru} = 0$ for all times, which we expect to hold also for the numerical solution produced by the interpolation

Table 4 Experiment 3, rotating hump: L^2-error of the solution of the *Galerkin projection scheme* (5.5) with Heun's method for different discretization parameters timestep τ (*rows*) and meshwidth h (*columns*)

$\tau \backslash h$	0.420	0.210	0.105	0.052	0.026
1.5707	1.85	1.87	1.94	1.88	2.33
0.7853	1.84	1.61	1.52	1.73	1.84
0.3926	1.83	1.71	1.01	0.56	0.51
0.1963	1.84	1.74	1.22	0.67	0.25
0.0997	1.84	1.78	1.50	0.86	0.34
0.0498	1.84	1.80	1.59	1.20	0.56
0.0249	1.85	1.81	1.62	1.28	0.81
0.0124	1.85	1.81	1.66	1.40	0.99
0.0062	1.85	1.82	1.67	1.43	1.10

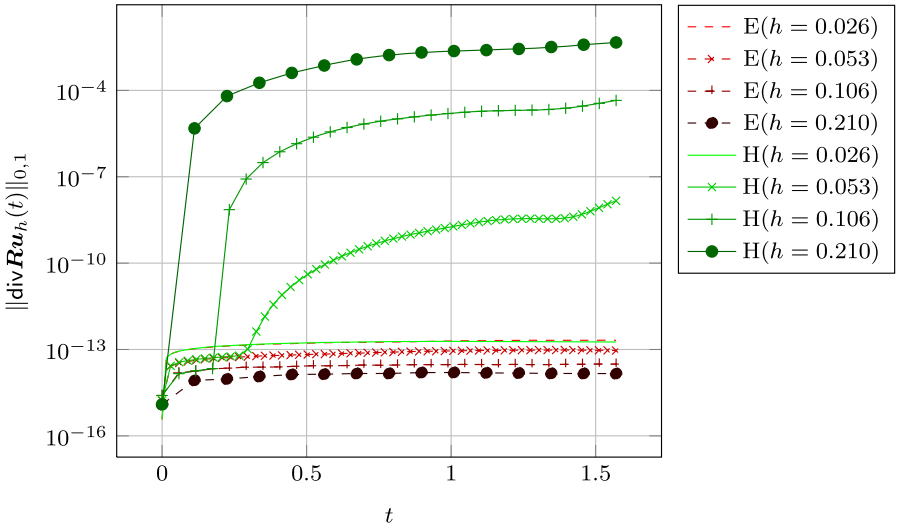

Fig. 6 Experiment 3: Behavior of $\|\mathrm{div}\boldsymbol{R}\boldsymbol{u}_h\|_{0,1}$ as a function of t, with $\boldsymbol{u}_h$ produced by the interpolation scheme with Heun's method (H) and explicit Euler method (E) on meshes with different mesh sizes for the time interval $[0, 0.5\pi]$

scheme. Yet, when using Heun's method for tracking vertex trajectories, this is only true for small timesteps and fine meshes as can be seen from Fig. 6. On the other hand, the scheme based on explicit Euler seems immune to "div-pollution".

We blame this puzzling observation on the fact that the approximate flow maps will not map Ω exactly onto itself; backward trajectories may leave the domain and there may be edges, whose image under the flow will be at least partly outside the fixed mesh. In our implementation of the interpolant $\Pi_h \bar{X}^*_{-\tau}\omega_h$ we simply ignore the contribution of such edges, thus destroying the closedness property, see Fig. 7. As long as ω_h has compact support away from $\partial\Omega$ this effect remains invisible. Yet, inevitable artificial diffusion will make $\operatorname{supp}\omega_h$ spread, reach $\partial\Omega$, and interpolation errors will pollute $d\omega_h$, see Fig. 6. Perversely, this happens for Heun's method but not in the case of the Euler method, because for the rotating flow the latter introduces

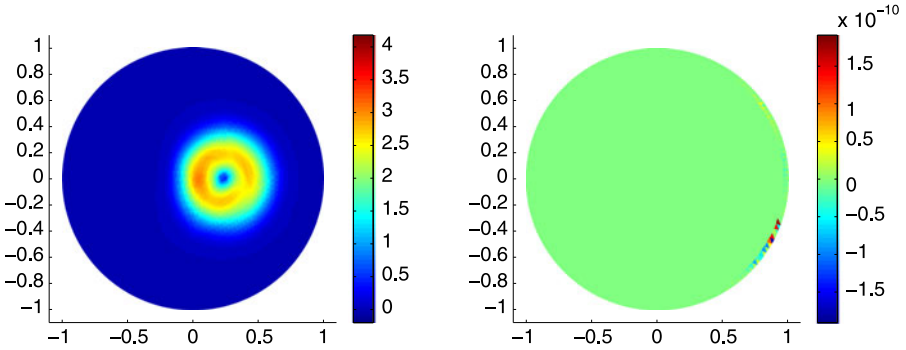

Fig. 7 Experiment 3: Plot of the modulus of $\boldsymbol{u}_h(0.5\pi)$ (*left*) and $\mathsf{div}\boldsymbol{R}\boldsymbol{u}_h(0.5\pi)$ (*right*), with $\boldsymbol{u}_h$ obtained by the interpolation scheme with Heun's method on a mesh with meshwidth $h = 0.0521$ and $\kappa = 0.8$. Note the "div-pollution" emerging close to $\partial\Omega$

a stronger drift towards the center, which completely offsets outward numerical diffusion.

References

1. Arnold, D.N., Falk, R.S., Winther, R.: Finite element exterior calculus, homological techniques, and applications. Acta Numer. **15**, 1–155 (2006)
2. Arnold, D.N., Falk, R.S., Winther, R.: Finite element exterior calculus: from Hodge theory to numerical stability. Bull. Am. Math. Soc. (New Ser.) **47**(2), 281–354 (2010)
3. Baker, M.D., Süli, E., Ware, A.F.: Stability and convergence of the spectral Lagrange-Galerkin method for mixed periodic/non-periodic convection-dominated diffusion problems. IMA J. Numer. Anal. **19**(4), 637–663 (1999)
4. Benson, D.J.: Computational methods in Lagrangian and Eulerian hydrocodes. Comput. Methods Appl. Mech. Eng. **99**(2–3), 235–394 (1992)
5. Bercovier, M., Pironneau, O., Sastri, V.: Finite elements and characteristics for some parabolic-hyperbolic problems. Appl. Math. Model. **7**(2), 89–96 (1983)
6. Bossavit, A.: In: Applied Differential Geometry (2005). http://butler.cc.tut.fi/~bossavit/BackupICM/Compendium.html
7. Bossavit, A.: Discretization of electromagnetic problems: the "generalized finite differences". In: Schilders, W.H.A., ter Maten, W.J.W. (eds.) Numerical Methods in Electromagnetics. Handbook of Numerical Analysis, vol. XIII, pp. 443–522. Elsevier, Amsterdam (2005)
8. Ciarlet, P.G.: The Finite Element Method for Elliptic Problems. Studies in Mathematics and Its Applications, vol. 4. North-Holland, Amsterdam (1978)
9. Dawson, J.M.: Particle simulation of plasmas. Rev. Mod. Phys. **55**(2), 403–447 (1983)
10. Douglas, J. Jr., Russell, T.F.: Numerical methods for convection-dominated diffusion problems based on combining the method of characteristics with finite element or finite difference procedures. SIAM J. Numer. Anal. **19**(5), 871–885 (1982)
11. Ewing, R.E., Wang, H.: A summary of numerical methods for time-dependent advection-dominated partial differential equations. J. Comput. Appl. Math. **128**(1–2), 423–445 (2001)
12. Ewing, R.E., Russell, T.F., Wheeler, M.F.: Convergence analysis of an approximation of miscible displacement in porous media by mixed finite elements and a modified method of characteristics. Comput. Methods Appl. Mech. Eng. **47**(1–2), 73–92 (1984)
13. Frankel, T.: The Geometry of Physics: An Introduction. Cambridge University Press, Cambridge (1998)
14. Gurtin, M.E.: An Introduction to Continuum Mechanics. Academic Press, San Diego (1981)
15. Hartman, P.: Ordinary Differential Equations. Wiley, New York (1964)

16. Hasbani, Y., Livne, E., Bercovier, M.: Finite elements and characteristics applied to advection-diffusion equations. Comput. Fluids **11**(2), 71–83 (1983)
17. Heumann, H., Hiptmair, R.: Convergence of lowest order semi-Lagrangian schemes. Report 2011-47, SAM, ETH Zürich (2011). Submitted to Found. Comp. Math.
18. Heumann, H., Hiptmair, R.: Eulerian and semi-Lagrangian methods for convection-diffusion for differential forms. Discrete Contin. Dyn. Syst. **29**(4), 1471–1495 (2011)
19. Heumann, H., Hiptmair, R.: Refined convergence theory for semi-Lagrangian schemes for pure advection. Technical report 2011-60, Seminar for Applied Mathematics, ETH Zürich (2011). http://www.sam.math.ethz.ch/reports/2011/60
20. Heumann, H., Hiptmair, R., Xu, J.: A semi-Lagrangian method for convection of differential forms. Technical report 2009-09, Seminar for Applied Mathematics, ETH Zürich (2009). http://www.sam.math.ethz.ch/reports/2009/09
21. Hiptmair, R.: Finite elements in computational electromagnetism. Acta Numer. **11**, 237–339 (2002)
22. Houston, P., Schwab, C., Süli, E.: Discontinuous hp-finite element methods for advection-diffusion-reaction problems. SIAM J. Numer. Anal. **39**(6), 2133–2163 (2002)
23. Hughes, T.J.R., Brooks, A.: A multidimensional upwind scheme with no crosswind diffusion. In: Finite Element Methods for Convection Dominated Flows. AMD, vol. 34, pp. 19–35. Am. Soc. Mech. Engrs., New York (1979)
24. Jack, R.O.: Convergence properties of Lagrangian-Galerkin method with and without exact integration. Technical report OUCL report 87/10, Oxford (1987)
25. Johnson, C.: A new approach to algorithms for convection problems which are based on exact transport + projection. Comput. Methods Appl. Mech. Eng. **100**(1), 45–62 (1992)
26. Lasaint, P., Raviart, P.-A.: On a finite element method for solving the neutron transport equation. In: In Proc. Sympos., Math. Res. Center, Univ. of Wisconsin-Madison, vol. 33, pp. 89–123. Academic Press, New York (1974)
27. Morton, K.W., Priestley, A., Süli, E.: Stability of the Lagrange-Galerkin method with nonexact integration. RAIRO Modél. Math. Anal. Numér. **22**(4), 625–653 (1988)
28. Morton, K.W., Süli, E.: Evolution-Galerkin methods and their supraconvergence. Numer. Math. **71**(3), 331–355 (1995)
29. Nédélec, J.-C.: Mixed finite elements in $\mathbf{R}^3$. Numer. Math. **35**(3), 315–341 (1980)
30. Nédélec, J.-C.: A new family of mixed finite elements in $\mathbf{R}^3$. Numer. Math. **50**(1), 57–81 (1986)
31. Pironneau, O.: On the transport-diffusion algorithm and its applications to the Navier-Stokes equations. Numer. Math. **38**(3), 309–332 (1981/1982)
32. Priestley, A.: Exact projections and the Lagrange-Galerkin method: a realistic alternative to quadrature. J. Comput. Phys. **112**(2), 316–333 (1994)
33. Reed, W.H., Hill, T.R.: Triangular mesh methods for the neutron transport equation. Tech. rep. LA-UR-73-479, Los Alamos National Laboratory, Los Alamos, NM (1973)
34. Rieben, R.N., White, D.A., Wallin, B.K., Solberg, J.M.: An arbitrary Lagrangian-Eulerian discretization of MHD on 3D unstructured grids. J. Comput. Phys. **226**(1), 534–570 (2007)
35. Scheja, G., Storch, U.: Lehrbuch der Algebra. Teil 2. Mathematische Leitfäden. Teubner, Stuttgart (1988)
36. Schwarz, G.: Hodge Decomposition—A Method for Solving Boundary Value Problems. Lecture Notes in Mathematics, vol. 1607. Springer, Berlin (1995)
37. Staniforth, A., Côté, J.: Semi-Lagrangian integration schemes for atmospheric models: a review. Mon. Weather Rev. **119**, 2206–2223 (1991)
38. Süli, E., Ware, A.: A spectral method of characteristics for hyperbolic problems. SIAM J. Numer. Anal. **28**(2), 423–445 (1991)